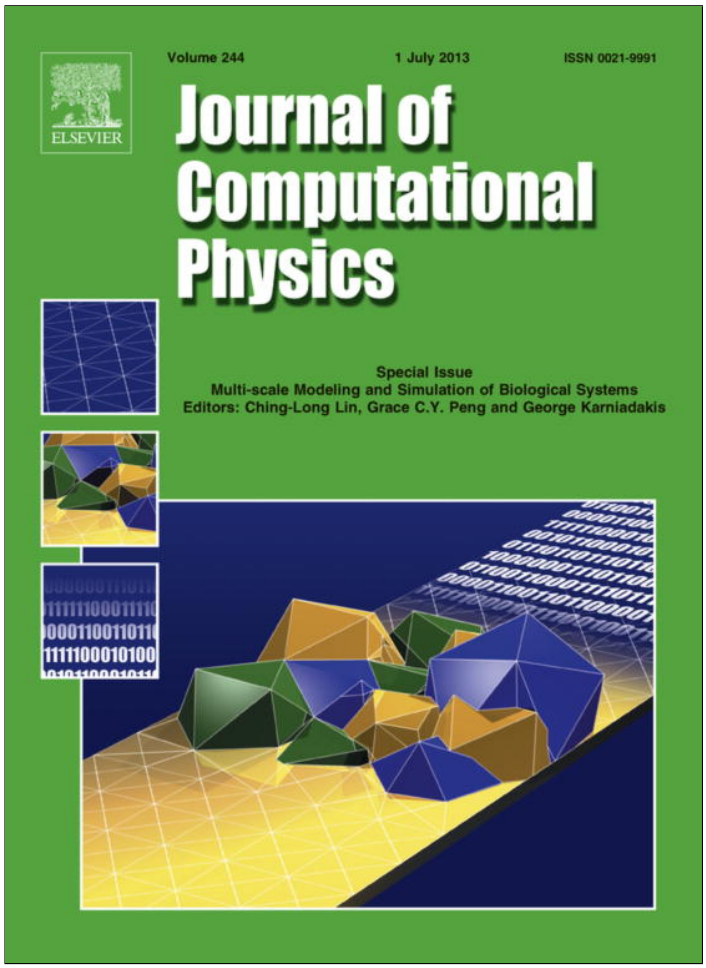

Journal of Computational Physics 244 (2013) 236–251

Contents lists available at SciVerse ScienceDirect

Journal of Computational Physics

journal homepage: www.elsevier.com/locate/jcp

Micromechanical simulations of biopolymer networks with finite elements

Christian J. Cyron [a], Kei W. Müller [a], Andreas R. Bausch [b], Wolfgang A. Wall [a,*]

[a] Institute for Computational Mechanics, Technische Universität München, Boltzmannstr. 15, D-85748 Garching, Germany
[b] Lehrstuhl für Zellphysik E27, Technische Universität München, Boltzmannstr. 15, D-85748 Garching, Germany

ARTICLE INFO

Article history:
Available online 21 January 2013

Keywords:
Brownian dynamics
Finite elements
Networks
Polymer physics

ABSTRACT

The mechanics of biological tissue is largely determined by the mechanics of biopolymer networks such as the extracellular matrix on cellular scale or the cytoskeleton on subcellular scale. Micromechanical simulations of biopolymer networks have thus attracted increasing interest in the last years. Here we introduce a simulation framework for biopolymer networks based on a finite element model of the filaments with a backward Euler time integration scheme. This approach surpasses previously published ones, especially those based on bead-spring models, by its sound theoretical foundation, a great flexibility, and at the same time an efficiency gain of approximately two orders of magnitude. Thereby it allows for addressing problems no previous numerical method could deal with, e.g., the micromechanical analysis of the viscoelastic moduli of crosslinked biopolymer networks in the low frequency regime or the analysis of the thermal equilibrium phases of such networks. By means of several examples it is discussed how this capacity can be exploited in multiscale simulations of biological tissue on cellular and subcellular scale.

1. Introduction

The mechanics of biological tissue is on both cellular and subcellular scale largely determined by the mechanics of biopolymer networks: on cellular scale, the cohesion between cells is ensured by the extracellular matrix, which is a biopolymer network consisting to a large extent of collagen fibers. On subcellular scale, the cytoskeleton, another biopolymer network mainly consisting of actin filaments, microtubules, and intermediate filaments, plays a crucial role for a variety of processes such as cell division, cell motility and mechanotransduction.

As a consequence, the mechanics of biopolymer networks has recently attracted rapidly increasing interest especially among biophysicists, bioengineers, biomedical engineers, mechanical engineers and material scientists. The great complexity and small length scale of these networks pose a great challenge for both experimental and theoretical investigation, which has given rise to the development of a variety of computational methods and models in this field. These can be divided into two main categories as illustrated in Fig. 1: macromechanical and micromechanical models.

In the first category, biopolymer networks are considered as macroscopic continua [1]. Their microstructure such as filament arrangement and interconnection is typically accounted for only by means of suitable nonlinear constitutive laws. By this first approach, large systems can be simulated at a low computational cost, however, at the prize that the simulation does not deliver detailed insights into processes on small length scales. This information has rather to be fed into the simulation algorithms in advance. As in life sciences simulations are often desired to provide information about exactly the very small length scales where experiments are especially difficult or even impossible, more detailed models are often required.

* Corresponding author.
E-mail address: wall@lnm.mw.tum.de (W.A. Wall).

0021-9991/$ - see front matter © 2012 Elsevier Inc. All rights reserved.
http://dx.doi.org/10.1016/j.jcp.2012.10.025

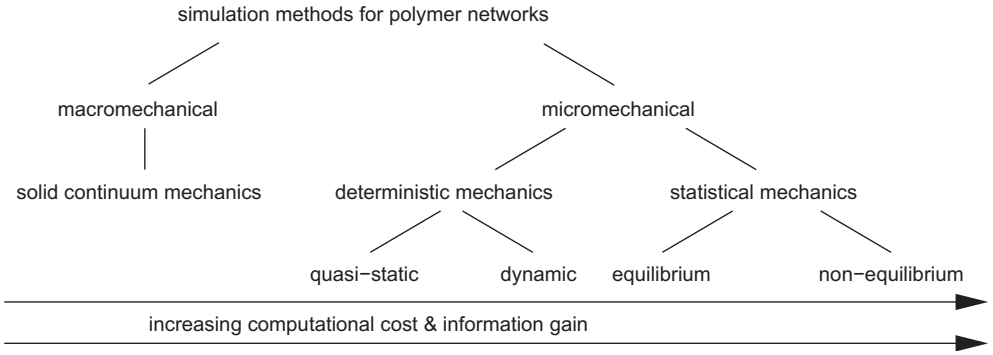

Fig. 1. Taxonomy of methods for the simulation of biopolymer networks: from left to right the computational cost is increasing, but also the information, which can be gained by the respective computational technique.

For this reason, analytical and numerical micromechanical models resolving the network down to the level of single filaments, i.e., to the length scale 1–10 μm, have been developed. They can be divided into those neglecting and those accounting for the stochastic thermal fluctuations to which filaments are exposed, according to the laws of statistical mechanics. If stochastic thermal fluctuations are neglected, filaments can be simulated on the basis of deterministic Newtonian mechanics in a quasi-static [2–4] or dynamic [5] way that include the molecular structure of the polymer to some degree. This approach can give insight into the mechanical properties of, for example, bundles of biopolymers and other dense aggreagates, when thermal fluctuations are not expected to play a dominant role. However, studies of the elastic properties of biopolymer networks demonstrate that neglecting thermal fluctuations is definitely not appropriate for networks composed of individual filaments. Thermal fluctuations are also central for decriptions of the interplay between mechanics and biochemistry ('mechano-chemistry') or the dynamic structural reorganisation in biopolymer networks, for example in the formation of lamellipodia.

Numerical simulation methods that attempt to capture thermal fluctuations can be grouped into those that aim to account only for the equilibrium thermodynamics and those addressing also non-equilibrium effects. In the first case, it is sufficient to capture the probability of all network configurations correctly in some way as it is done for example in Metropolis-Monte-Carlo models [6] without paying major attention to transition processes and probabilities between these configurations. In the second case, also the dynamical evolution of networks is captured. To this end, one typically employs methods based on the theory of Brownian dynamics and different kinds of filament discretizations such as bead-spring models [7,8], rods-on-string-models [9] or worm-like-chain segment models [10].

In simulation studies of networks of highly flexible polymers, such as rubber, the particular details of the polymer discretization are less important and any of these models can be used. The reason is that the key physical properties of these systems can be expressed in terms of power-law scaling relations, such as the dependence of the elastic moduli of the network on cross-link and monomer density. These scaling relations have been shown to be independent of the detailed properties of the monomers composing the polymer. However, for solutions of biopolymers, such as F-actin, 'universality' of important physical properties cannot be taken for granted and the details of the polymer discretization play a crucial role. For example, F-actin bundles are strongly affected by their chirality: it determines the diameter of F-actin bundles. Definite chirality is in fact the hallmark of biomolecules in general, wheras the numerical models mentioned above lack material triads and are therefore inherently non-chiral. Not only does this limit their capacity to capture biochemistry and mechanochemistry of biopolymers correctly, but it even prevents them from capturing essential mechanical features such as torsion and anisotropic bending stiffness. So far proposed extensions of the above discretizations by material triads in order to account for these features result in inefficient algorithms, which partially even suffer from numerical instability in case of general deformation owing to singularities [11–13].

Not only in this respect do the above mentioned polymer discretizations exhibit severe deficiencies, but also with respect to computational performance. Especially, classical bead-spring models with explicit time integration – which are the state of the art in computational polymer physics at the moment – suffer from an excessive computationl cost rendering the simulation of complex networks on the biologically most relevant time scale $10–10^3$ s impossible [7,8]. So far proposed remedies in order to reduce the computational cost of state-of-the-art methods such as inextensibility contraints [14] go along with significant theoretical intricacies and the loss of the capacity to capture certain physical phenomena such as axial stretching.

Summarizing the above facts, one can say that there is a significant need for micromechanical computer simulations of crosslinked biopolymer networks including non-equilibrium statistical mechanics and chirality of biopolymers on the length scale 1–10 μm and time scale $10–10^3$ s, but no known method by which such simulations can be performed at an acceptable computational cost.

In this article we propose such a method. It is based on a micromechanical continuum model of biopolymer networks which is pointed out in detail in Section 2. Section 2 essentially summarizes widely known facts about micromechanical models of biopolymer networks. It may be understood as an introduction for the reader not yet familiar with this field and skipped by the others. In Sections 3–5 it is pointed out how finite element simulations of biopolymer networks can

be conducted on the basis of the model described in Section 2. After a short discussion of the application of such simulations to multiscale problems, the capacity and performance of the proposed approach are illustrated by means of several numerical examples in Section 7.

2. Micromechanical continuum model of biopolymer networks

Biopolymer networks are formed by three main constituents: polymer filaments, crosslinker molecules (referred to also as 'linkers' in the following) which connect these filaments by transient chemical bonds, and a background fluid into which filaments and linkers are embedded. In Fig. 2, some examples of biopolymer networks consisting of actin filaments with different types and concentrations of crosslinker molecules are depicted. In the pictures only the filaments are clearly visible. The background fluid is typically an aqueous solution and therefore nearly transparent. The size of the linkers ranges on the nanometer scale so that they cannot be seen on the images in Fig. 2, which depict a sector of some microns edge length, respectively. The variety of completely different network architectures which can be formed by one and the same kind of filament just by the application of different linkers is remarkable.

The first important question is how to model the three main constituents of biopolymer networks in view of their small size. It is well-known that the behaviour of atoms as well as of any system constituted by atoms can be predicted in an accurate manner by the application of the laws of quantum mechanics to the entire system. However, the tremendous complexity of the resulting equations renders it impossible to pursue that strategy when trying to simulate systems consisting of more than just some dozens of atoms. To overcome that problem, one often resorts to molecular dynamics (MD) simulations, where effects of quantum physics are not considered explicitly, and single atoms or small packages of atoms are the smallest units. These are modeled on the basis of Newtonian mechanics, and their equations of motion typically account for potentials due to bonds between neighbouring units, non-bonded potentials as well as potentials originating from coulombic forces. Although MD models are much more efficient than quantum mechanical simulations, even an MD simulation of a minor biopolymer network on a time scale relevant for cell and tissue mechanics would by far exceed the computational resources available at the moment. On the other hand, the mechanics of biopolymer networks is primarily governed by deformations on the length scale of single filaments, which are typically some micrometers long. On this length scale, it is well-known from microfluidics as well as experimental polymer physics that continuum models already apply. Linkers are typically much smaller than filaments so that modeling them accurately by similar techniques may be more difficult. However, for reasons discussed below also for linkers a continuum model is expected to be sufficient when focussing on the mechanics of whole networks rather than of single linkers. The coarse-graining step from MD models to continuum models goes along with a vast reduction of the computational cost enabling even the simulation of entire biopolymer networks. Yet the essential information about micromechanical processes in the network on the level of single filaments is still kept. Thus, such a micromechanical continuum approach provides an excellent trade-off between computational cost and information gain and will be developed in detail in the following Sections 2.1, 2.2 and 2.3.

2.1. Fluid

From microfluidics it is well-known that a continuum model based on the Navier–Stokes equations is suitable for fluid volumes down to the micrometer length scale relevant for biopolymer networks. Modeling the fluid in these networks, one is confronted with two major difficulties: first, on the length scale of biopolymers stochastic thermal fluctuations according to the laws of statistical mechanics affect the fluid velocity field perceptibly; second, the fluid dynamics is affected by complex fluid–structure interactions with all the filaments and linkers in the network. These two effects can be accounted for in detail only at a considerable computational cost. Therefore various simplifications are common in polymer physics (cf. [16,17,7,8]): Due to the small length scale, low velocities and high viscosities, Reynolds and Mach numbers are usually small

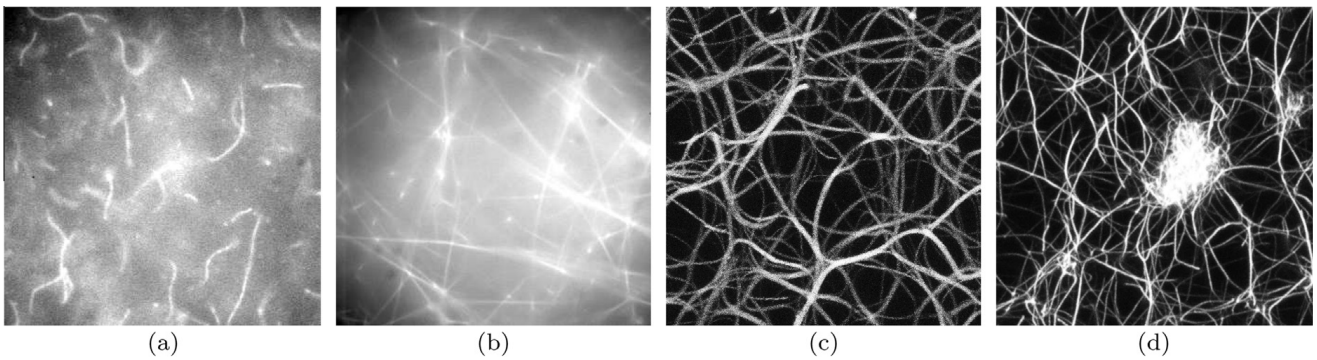

Fig. 2. Examples for biopolymer networks in vitro: (a) actin-HMM network ($52\mu m \times 52\mu m$), (b) actin-fascin bundle network (52 μm × 52 μm), (c) actin-filamin bundle network (60 μm × 60 μm) [15], (d) actin cluster (41 μm × 41 μm) [15].

in biopolymer networks. Thus a linearized version of the incompressible Navier–Stokes equations can be applied [17] so that the fluid velocity field can be separated into a deterministic part and a stochastic part owing to the thermal fluctuations. Because of the very small diameter and total volume fraction of filaments and linkers in the whole network (e.g., in a $4\mu M$ actin network the filament diameter is 5 nm and the volume fraction 6.5 %), the effect of the filament and linker motion on the deterministic part of the fluid velocity field is small. Therefore the deterministic part of the fluid velocity field is computed initially on the basis of the boundary conditions of the simulation volume only, and the forces and moments it entails for filaments and linkers are captured by simple friction coefficients assuming a Newtonian fluid. The stochastic part of the fluid velocity field has then never to be computed explicitly, because it causes no effective drag, but only a stochastic excitation independent on fluid, filament and linker motion. This excitation, however, can be computed immediately from the friction coefficients of filaments and linkers according to the fluctuation–dissipation theorem [16]. In general, the deterministic part of the fluid velocity field can be computed by standard methods such as the finite element or finite volume method. In practice, not even this may be necessary as it is often either zero or a simple shear flow which can be calculated analytically without any discretization. Therefore the treatment of the fluid velocity field will not be discussed in any more detail below, and it will rather be assumed to be given.

More sophisticated models for the fluid including the fluid–structure interactions in one or another way may be an interesting avenue of future research. These may either be based on a simple consideration of the Navier–Stokes equations' characteristics similar to the Oseen- or Rotne-Prager tensors well-known in polymer physics [18,19] or on more sophisticated ideas such as presented in [20] or [21].

2.2. Filaments

Force transmission in biopolymer networks is usually assumed to occur predominatly via the filaments. These are rod-like structures whose length typically ranges between 100 nm and 100 μm and whose slenderness ratio may reach from 10 to far above 1000. From a variety of experiments (e.g., [22–25]) it is well-known that not only the fluid on that length scale can be modeled as a mechanical continuum, but that also rod-like structures such as biopolymers can be considered as mechanical continua with axial, bending and torsion stiffness so that classical beam theories such as the one of Euler and Bernoulli can be employed [26]. Thus the dynamics of filaments has not to be modeled on the basis of quantum mechanics or molecular dynamics (MD), but rather a coarse grained continuum model can be used instead of an atomistic or molecular one. Employing a continuum model, the equation of motion of a filament, i.e. its balance of linear and angular momentum, comprises the following quantities.

First, viscous forces $\boldsymbol{f}_{visc}$ and moments $\boldsymbol{m}_{visc}$ account for the damping the filament experiences moving through the fluid. It is underlined that in the model developed in the following only such external friction is considered and not any kind of internal friction in the filaments as discussed in [27]. In polymer physics, such internal friction is typically assumed to play only a minor role, and if necessary it can be added to the approach developed below by only some minor modifications.

Second, stochastic forces $\boldsymbol{f}_{stoch}$ and moments $\boldsymbol{m}_{stoch}$ capture the stochastic excitation of the filament by the thermal fluctuations in the fluid. They are related to the viscous forces and moments by the fluctuation–dissipation theorem as already mentioned in Section 2.1 and discussed in more detail below.

Third, miscellaneous deterministic interactions between a filament and either other filaments, linkers or the fluid are summed up in the deterministic external forces $\boldsymbol{f}_{ext}$ and the moments $\boldsymbol{m}_{ext}$. These miscellaneous interactions may be long range interactions, e.g., owing to electrostatic potentials, or short range interactions, e.g., due to contact between different filaments or linkers or due to chemical bonds.

As the mass of a body scales cubically with its size, but its surface only quadratically, inertia can usually be neglected as compared to friction on the small length scale of single filaments in a polymer network so that dynamics can be modeled by a differential equation of only first order in time. It should be noted that by this modeling assumption the applicability of the present model is in principle limited towards larger length scales, although this limitation can typically be disregarded for the simulation of biopolymer networks. Mathematically, viscous forces and moments can typically be modeled as smooth functions, miscellaneous external forces and moments as smooth functions in case of long range interactions and as point loads in case of short range interactions. For the stochastic excitations $\boldsymbol{f}_{stoch}$ and $\boldsymbol{m}_{stoch}$, the situation is more difficult: physically, they are caused by the random thermal motion of a large number of particles in the surrounding fluid which interact with the filament for example by collisions or transient chemical bindings. Due to the tremendous number and small size of these particles as well as the approximate pairwise independence of their trajectories, the resulting stochastic excitation can be modeled by functions piecewise C^0-continuous on intervals of the length $\Delta\xi \to 0$. Precisely, one models the stochastic excitation by so-called space–time white noise functions as discussed in more detail below. This turns the equation of motion into a stochastic partial differential equation (SPDE), which is usually referred to as Brownian equation of motion.

A key question for the simulation of biopolymer networks is how to discretize this SPDE in space and time efficiently. Despite the dominant role of Brownian dynamics (BD) in polymer physics [16], still purely heuristic models such as bead-spring and bead-rod models with explicit Euler time integration are most common in computational polymer physics. These models capture the essential features of BD correctly, but are based on physical intuition rather than on a rigorous mathematical foundation. Moreover, they either require non-physical constraints entailing significant intricacies and rendering the simulation of certain phenomena such as axial extension of filaments impossible [14], or they suffer from serious performance problems when employed for the simulation of large systems [7,8]. To overcome these severe deficiencies,

a finite element method for the simulation of polymers and other microscopic rod-like continua was developed in [28–30]. This method is derived from first principles of Newtonian and statistical mechanics in a stringent mathematical way and at the same time exhibits a superior performance. However, so far, it has been applied only to the simulation of single filaments rather than of whole biopolymer networks. In this article we will briefly recall its most important features in Section 3 and then demonstrate how to make use of it in simulations of biopolymer networks.

2.3. Linkers

Filaments in biopolymer networks may be connected mechanically by crosslinking molecules, to which we will refer in the following also as linkers. Linkers are typically between 5 nm (fascin, [31]) and 100 nm (filamin, [32]) long and thus much smaller than the filaments in the networks, which are most often at least some microns, in experiments even several tens of microns long. They can form up to two chemical bonds with so-called binding sites on the filaments. Hence, we may distinguish between three states of linkers:

(I) free (i.e., without any chemical bond to any filament),
(II) singly bound (i.e., with one chemical bond to some filament),
(III) doubly bound (i.e., with two chemical bonds to filaments).

Free linkers are solved as particles in the fluid and not expected to take part in the force transmission in the network perceptibly. Rather they represent a pool of particles which can form chemical bonds with filaments close by and thereby change to a state of greater mechanical importance. Therefore only the position of these particles matters, because it is the basis for the decision which filaments are close enough to establish a chemical bond. Neglecting their internal structure fluctuations, they are thus modeled as point-shaped particles moving through the network stochastically according to the laws of Newtonian and statistical mechanics.

Linkers which are already bound to one filament are not supposed to perceptibly affect the network mechanics, either. Excessive amounts of such linkers may change the effective stiffness of the filament to which they are attached, but even this effect is expected to be negligible in most cases. Therefore such linkers are still modeled as point-shaped particles, but not in stochastic Brownian motion, but rather attached to a filament at a certain point. If they come close enough to another binding site they may form a second chemical bond and become doubly bound linkers.

Linkers having established chemical bonds to two filaments can be modeled as rod-like continua coupling these filaments with an effective stretching, shear, torsion and bending stiffness. Like the filaments themselves, they are subject to viscous damping and stochastic excitation from the fluid. Indeed, this rough model is not expected to resolve the internal deformation of linkers accurately. However, on the basis of the data available about linkers at the moment, this seems impossible anyway: the small size of linkers significantly complicates experimental studies of their mechanical properties, and so far this lack of experimental data has been compensated only partially by data from MD simulations. Once more information will be available about linkers in the future, the here introduced linker model can be refined easily and without major implications for the filament and fluid model.

Altogether, in a computer simulation based on the above linker model, for free and singly bound linkers only the positions have to be tracked, whereas for doubly bound linkers also the force transmission they allow between filaments has to be captured. How to do so, is pointed out exactly in Section 4.

2.4. Interactions

Not only fluid, filaments, and linkers have to be modeled, but rather also the interactions between them. As discussed above, the viscous interactions between fluid and filaments can be captured by viscous and stochastic forces and moments in the equation of motion of the filaments. In addition to that also electrostatic interactions between the fluid and filaments may arise because filaments are in general charged (e.g., actin filaments exhibit a linear charge density of $4e/nm$ [33]). By this charge filaments may interact with ions in the surrounding fluid. A great number of models for this aqueous electrostatics has been described in the literature. Here we abstain from any detailed discussion and simply assume that this effect can be accounted for by ionic correction factors, which can be incorporated similarly to shear correction factors in classical beam mechanics in the effective stiffness of filaments and do not require any further numerical modeling effort. The same as for interactions between filaments and fluid is assumed, of course, also for interactions between linkers and fluid. Thus, only interactions between filaments and linkers remain to be discussed. In experiments so far two main types of such interactions have been observed:

(I) chemical interactions,
(II) contact interactions.

Chemical interactions lead to the formation of chemical bonds between linkers and filaments and thereby turn free linkers into singly bound ones and singly bound linkers into doubly bound ones. These bonds are in general only temporary and disaggregate stochastically after a while owing to thermal fluctuations. Such unbinding events turn doubly bound linkers

into singly bound ones and singly bound linkers into free ones. Contact interactions play an important role when filaments and linkers come close to each other and prevent them from overlapping. Direct electrostatic interactions between filaments and linkers except for those in chemical and contact interactions are neglected in this article, because their impact is typically strongly limited by the ionic patterns in the fluid shielding charged filaments and linkers. In certain special cases such interactions may matter,e.g., for the diffusion of charged particles in polymer networks [34] or also for the network architecture in the presence of certain linker types [35], but a discussion of these cases would go beyond the scope of this paper.

2.5. Summary of modeling

Biopolymer networks can be modeled on a micromechanical scale as complex systems consisting of three main constituents: a fluid, filaments and linkers. These can be modeled as continua, respectively. Often the fluid can be handled by standard methods and even without a discretization. In opposition to that, filaments, linkers and the interactions between them have to be considered explicitly in a numerical simulation. How to do so will be discussed in detail in the Sections 3–5.

3. Numerical model of filaments

The most important constituent of biopolymer networks are the polymers themselves, for which a continuum model was developed in [28–30]. This cornerstone of the model will be briefly recapitulated in the following: biopolymers of length L can be modeled as rod-like Cosserat continua, i.e. at a point in time $t \in [0; t_{max}]$ as curves in $\mathbb{R}^3 \times \mathrm{SO}(3)$ with curve parameter $\xi \in [0; L]$ where SO(3) is the special orthogonal group. In a rod-like Cosserat continuum to each material curve point ξ at a certain point in time t both a spatial point $\boldsymbol{x}(\xi, t) \in \mathbb{R}^3$ and a triad $\boldsymbol{R}(\xi, t) \in \mathrm{SO}(3)$ is assigned. The curve $\boldsymbol{x}$ represents the center line of the polymer backbone, and the columns of the triad $\boldsymbol{R}(\xi, t)$ represent the three principal axes of the cross section at the point $\boldsymbol{x}(\xi, t)$ of this center line. The triad $\boldsymbol{R}((\xi, t))$ is equivalent to some orientation vector $\boldsymbol{\theta}(\xi, t) \in \mathbb{R}^3$ so that the motion of a single biopolymer may be completely characterized by the two functions

$$\boldsymbol{x} : [0; L] \times [0; t_{max}] \to \mathbb{R}^3, \quad (\xi, t) \mapsto \boldsymbol{x}(\xi, t), \tag{1}$$

$$\boldsymbol{\theta} : [0; L] \times [0; t_{max}] \to \mathbb{R}^3, \quad (\xi, t) \mapsto \boldsymbol{\theta}(\xi, t). \tag{2}$$

The functions $\boldsymbol{x}$ and $\boldsymbol{\theta}$ are the solution to the equations of motion

$$\boldsymbol{f}_{el}(\boldsymbol{x}, \boldsymbol{\theta}, \xi, t) + \boldsymbol{f}_{visc}(\boldsymbol{x}, \boldsymbol{\theta}, \xi, t) = \boldsymbol{f}_{ext}(\boldsymbol{x}, \xi, t) + \boldsymbol{f}_{stoch}(\boldsymbol{x}, \boldsymbol{\theta}, \xi, t), \tag{3a}$$

$$\boldsymbol{m}_{el}(\boldsymbol{x}, \boldsymbol{\theta}, \xi, t) + \boldsymbol{m}_{visc}(\boldsymbol{x}, \boldsymbol{\theta}, \xi, t) = \boldsymbol{m}_{ext}(\boldsymbol{x}, \xi, t) + \boldsymbol{m}_{stoch}(\boldsymbol{x}, \boldsymbol{\theta}, \xi, t) + \boldsymbol{x}'(\xi, t) \times \boldsymbol{q}_{el}(\boldsymbol{x}, \boldsymbol{\theta}, \xi, t). \tag{3b}$$

Here $\boldsymbol{f}_{visc}, \boldsymbol{m}_{visc}, \boldsymbol{f}_{stoch}, \boldsymbol{m}_{stoch}, \boldsymbol{f}_{ext}, \boldsymbol{m}_{ext}$ are the viscous, stochastic and deterministic external force and moment loads per unit length. Eq. (3a) represents the balance of linear momentum and Eq. (3b) the balance of angular momentum. Partial derivatives with respect to the curve parameter ξ are denoted by a prime and partial derivatives in time will be denoted in the following by an overdot. The elastic section force $\boldsymbol{q}_{el}$ and the elastic section moment are, as usual for one-dimensional continua, defined as the integral and resulting moment of the internal stresses. The derivatives of the section force and moment with respect to ξ are $\boldsymbol{f}_{el}$ and $\boldsymbol{m}_{el}$, respectively. Assuming a Newtonian fluid, the viscous forces and moments can be computed by

$$\boldsymbol{f}_{visc} = \boldsymbol{c}_t[\dot{\boldsymbol{x}} - \boldsymbol{v}(\boldsymbol{x})], \tag{4a}$$

$$\boldsymbol{m}_{visc} = \boldsymbol{c}_r\left[\dot{\boldsymbol{\theta}} - \boldsymbol{\omega}(\boldsymbol{x})\right]. \tag{4b}$$

Here $\boldsymbol{v}$ and $\boldsymbol{\omega}$ are the translational and rotational velocity field of the background fluid, and $\boldsymbol{c}_t$ and $\boldsymbol{c}_r$ are the translational and rotational damping tensors. According to the fluctuation dissipation theorem, the stochastic forces and moments are then Gaussian random variables with

$$\langle \boldsymbol{f}_{stoch} \rangle = 0, \tag{5a}$$

$$\langle \boldsymbol{f}_{stoch} \otimes \boldsymbol{f}_{stoch} \rangle = 2k_B T \boldsymbol{c}_t \delta_{tt^*} \delta_{\xi\xi^*}, \tag{5b}$$

$$\langle \boldsymbol{m}_{stoch} \rangle = 0, \tag{6a}$$

$$\langle \boldsymbol{m}_{stoch} \otimes \boldsymbol{m}_{stoch} \rangle = 2k_B T \boldsymbol{c}_r \delta_{tt^*} \delta_{\xi\xi^*}, \tag{6b}$$

where $\langle . \rangle$ denotes an average, k_B the Boltzmann constant, t, t^* and ξ, ξ^* represent in general different points in time and space, respectively, and δ_{tt^*} is the Dirac-function with argument $t - t^*$. As pointed out in detail in [28–30], (3) can be discretized by nonlinear beam elements of reference length h in space and a backward Euler scheme in time, which allows for a simple and highly efficient simulation of the filaments in biopolymer networks.

4. Numerical model of linkers

4.1. General

For setting up a numerical model of linkers, some initial definitions are helpful. First of all, the distance between the two binding domains of a linker is assumed to range in the interval $[R_{cl} - \Delta R_{cl}; R_{cl} + \Delta R_{cl}]$. Here, R_{cl} is the characteristic distance between the two binding domains and ΔR_{cl} a tolerance accounting for the fact that the actual distance between the binding domains may vary over time, e.g., owing to minor thermal fluctuations of the linker position, orientation and configuration. Values of R_{cl} are presented in Table 1 for several linkers common in biopolymer networks.

The position of the point in the middle between the two binding domains is denoted by $\boldsymbol{x}_{cl,c}$. In general, the lower index $(.)_{cl}$ is reserved in this article to mark properties of and quantities related to linkers. Then linkers can be modeled in computer simulations depending on their current state as follows.

4.2. Free linkers

As discussed in Section 2.3, for a free linker it is enough to keep track of its position in space so that it can be modeled as a point-like particle with position $\boldsymbol{x}_{cl,c}$ and friction coefficient ζ_{cl}. In general, its equation of motion is then given by

$$\boldsymbol{f}_{visc,cl}(\boldsymbol{x}_{cl,c}, \dot{\boldsymbol{x}}_{cl,c}, t) = \boldsymbol{f}_{ext,cl}(\boldsymbol{x}_{cl,c}, t) + \boldsymbol{f}_{stoch,cl}(\boldsymbol{x}_{cl,c}, t), \tag{7}$$

where $\boldsymbol{f}_{visc,cl}$ is the viscous force the linker experiences moving through the background fluid, $\boldsymbol{f}_{ext,cl}$ is the sum of external deterministic forces the linker is subject to, e.g., as a consequence of force fields, and $\boldsymbol{f}_{stoch,cl}$ is the stochastic thermal force exerted by the thermal bath into which it is embedded. In a Newtonian fluid, the viscous force is simply given by

$$\boldsymbol{f}_{visc,cl} = \zeta_{cl}\dot{\boldsymbol{x}}_{cl,c}, \tag{8}$$

and the stochastic force is then according to the fluctuation–dissipation theorem

$$\boldsymbol{f}_{stoch,cl} = \sqrt{2k_B T\zeta_{cl}}\dot{\mathcal{W}}_{\boldsymbol{cl}}(t) \tag{9}$$

with the standard Wiener process $\mathcal{W}_{cl}(t)$. For the computation of the position $\boldsymbol{x}_{cl,c}$, a simple backward Euler scheme can be applied to (7) in general. In the special case of a constant friction coefficient and negligible external deterministic forces, the position increment in a time step is just the respective increment of the Wiener process $\mathcal{W}_{cl}(t)$ times a constant factor.

4.3. Singly bound linkers

As discussed in Section 2.3, also for singly bound linkers it is enough to keep track of their position, because they are not assumed to play a major role for force transmission and mechanics of biopolymer networks. However, in opposition to the position of free linkers, theirs is not governend by stochastic, thermal motion, but rather by the motion of the filament they are bound to. Thus we do not compute the position of singly bound linkers explicitly, but simply assume that they follow the binding site to which they are attached without affecting the dynamics of the filament on which this binding site is situated.

4.4. Doubly bound linkers

Doubly bound linkers form elastic and often rather stiff connections between two filament binding sites. Anyway, an extensional stiffness has to be attributed to this mechanical connection. Depending on whether experiments suggest either a finite or a negligible bending and torsion stiffness, doubly bound linkers are therefore represented by either finite beam elements or simple truss elements. The reference length of these elements may be set equal to the distance between the two filament binding sites connected by the linker at the point in time when the connection is established. In addition to stiffness, so-called active linkers (motor proteins) may have an additional characteristic property which is the force or moment they can actively exert on the filaments they connect in order to shift or turn them against each other. This property of active linkers is well-known to play a key role in the rearrangement of the cytoskeleton during cell migration so that active linkers in general play an important role in cell biology. A variety of fundamental properties of biopolymer networks, however, can already be studied only by means of passive linkers. Therefore, the focus of this article is limited for simplicity on the latter ones, leaving the issue of active linkers for future work.

Table 1
Biologically especially relevant crosslinker molecules, the characteristic distance R_{cl} they bridge, and references to more information in the literature. HMM (heavy meromyosin) is a fragment of the motor molecule myosin II and is often used as a crosslinker molecule in vitro, but not in vivo."

Crosslinker type	HMM	α-Actinin	Filamin	Fascin	Espin
R_{cl}	40 nm	40 nm	98 nm	5 nm	5 nm
Reference	[36]	[37]	[32]	[31]	[31]

4.5. Discussion

Using the above linker model in computer simulations, an important question is how to determine the required numerical parameters such as the characteristic binding length R_{cl} or the stiffness of the linkers. In principle, there are two ways how to determine these quantities: experimentally (e.g. [38]) or by MD simulations (e.g., [39,40]). The considerable difficulties of single-molecule experiments on the one hand and the fast-growing power of computational methods on the other hand gives rise to the expectation that data gained by MD simulations will be especially relevant in the future.

Finally, it seems worth comparing the above linker model to previously published models. So far, mainly two linker models have been studied in the literature: in the first model [5,3,4], all filaments are connected by a linker as soon as they get close enough to each other. Motion and position of unbound linkers are not simulated explicitly. The number of linkers can be limited by some upper bound or left unlimited. In the second model [7,8], also free and singly bound linkers are simulated.

The first way of modeling linkers can obviously not account for linker diffusion. As long as a certain maximal number of links has not yet been exceeded, linkers are just assumed to be available wherever filaments come close enough to each other to be connected. In reality, however, the motion and therefore also availability of linkers at a certain point in space is governed and also limited by thermal diffusion forces, kinematic constraints, which, e.g., prevent linkers from intersecting with filaments or other linkers, and sometimes also electrostatic potentials. In certain cases, one may not be interested in a detailed simulation of the interplay between these factors and then the first linker model is completely sufficient. However, a variety of highly important physical effects cannot be studied at all with this model: for example surveying the non-equilibrium thermodynamics of polymer networks usually requires a fairly accurate model of the dynamics of all main constituents of the network, especially of both the filaments and the linkers. Kinematic constraints delaying or even suppressing the motion of linkers may crucially affect the way filaments can interact with each other so that the computer simulation of non-equilibrium thermodynamics is in general impossible using the first linker model. In addition to that, also certain equilibrium effects go beyond the scope of this first model: for example, the attractive potential of filament binding sites directly governs the number of crosslinks in the network. This potential can only be determined by computer simulation if the competition between linker binding energy and linker diffusion is simulated explicitely.

The linker model introduced in Section 4 is obviously of the second type and offers therefore a powerful basis for the simulation of both equilibrium and non-equilibrium processes.

5. Numerical model of interactions between filaments and linkers

5.1. Chemical bonds

Filaments and linkers may interact with each other by chemical bonds which transmit forces and moments. In the following, we will assume that such bonds arise only between one filament and one linker, respectively. Direct chemical bonds between two filaments or two linkers will not be discussed as in biopolymer networks such bonds are typically assumed either not to arise at all or not to matter. It is emphasized, however, that the quantitative considerations below about bonds between one filament and one linker can be directly applied also to chemical bonds between two filaments or two linkers if this required in some special case in the future.

To form a chemical bond, a linker L and a free filament binding site F have to be sufficiently close to each other, i.e., the linker has to be within the so-called reaction volume V_{react} of the binding site. Once this is the case, both molecules can form a bond if they reach a proper relative position and orientation. In a very short time interval Δt, where the probability of multiple binding and unbinding events is negligible, this can be modeled by a Poisson process with a so-called on-rate $k_{react,on}$, and the probability for binding can be computed by

$$p_{on} = 1 - \exp\left(-k_{react,on}\Delta t\right). \tag{10}$$

Similarly, unbinding of a linker already bound to a filament happens with an off-rate $k_{react,off}$ and the probability

$$p_{off} = 1 - \exp\left(-k_{react,off}\Delta t\right). \tag{11}$$

In computer simulations based on the method introduced in this article, filament and linker positions are known at each point in time. Thus for a numerical model of chemical interactions between filaments and linkers, one just has to define the position of the binding sites on the filaments and their respective reaction volume.

In principle, a binding site may be any point on the filament. In reality, binding sites are usually periodically distributed over filaments with a characteristic distance h_{bind}. If filaments are discretized with finite elements, the simplest way of modeling binding sites is setting h_{bind} equal to the finite element discretization length h and defining the finite element nodes as the binding sites of the filament. This allows for modeling doubly bound linkers just as finite beam or truss elements connecting two already existing nodes in the filament discretization. Indeed, this simple model is employed in all the examples discussed in Section 7.

Modeling the reaction volume is possible in various ways. In view of Section 4, it seems reasonable assuming that free linkers can react with binding sites, if the distance between the linker center $\boldsymbol{x}_{cl,c}$ and the binding site ranges in the interval $[(R_{cl} - \Delta R_{cl})/2; (R_{cl} + \Delta R_{cl})/2]$. Singly bound linkers on the other hand can bind to another binding site only if the distance of

this binding site and the one they are already attached to ranges in the interval $[R_{cl} - \Delta R_{cl}; R_{cl} + \Delta R_{cl}]$. By means of these two distance criteria one can decide whether a linker is in the reaction volume of a binding site. If so, the calculation of the binding probability between both is possible by (10) for a simulation time step of length Δt.

This model can be extended easily by additional geometric constraints refining the definition of the reaction volume. A comprehensive discussion of such constraints would go beyond the scope of this paper, however, at least one example seems worth being discussed: it is well-known that certain types of linkers can connect only filaments in certain relative orientations. The linker fascin, e.g., can link only almost parallel filaments [41], whereas the linker alpha-actinin is flexible and rather insensitive towards the orientation of the linked filaments [41]. This can be modeled by a simple orientation constraint: singly bound linkers are assumed to be in the reaction volume of a free binding site only if the angle between the filament on which this binding site is situated and the filament to which the linker is already attached to ranges in the interval $[\phi - \Delta\phi; \phi + \Delta\phi]$. Here ϕ may be considered as preferred binding angle and $\Delta\phi$ as tolerance around it. The angle between the filaments can be computed in a finite element model either from the triads representing the cross section orientation of the filaments or alternatively from the tangents to the three dimensional curves representing their neutral lines. Both ways are expected to lead to almost identical results as shear deformation is usually negligible due to the high slenderness ratios of typical biopolymers.

For simulations, the parameters $k_{react,on}$ and $k_{react,off}$ have to be specified. Various data sources can be used to this end. The most important one is experiments such as presented in [42,43] where the on- and off-rates k_{on} and k_{off} of the bimolecular reaction

$$L + F \underset{k_{off}}{\overset{k_{on}}{\rightleftharpoons}} LF \tag{12}$$

are determined. Here LF is the species of linkers bound to a filament binding site. Denoting the molar concentration of a species by $[.]$, the number of binding and unbinding events per unit time and volume is given by definition of the on- and off-rates by $k_{on}[L][F]$ and $k_{off}[LF]$, respectively [26]. From the experimentally determined k_{on}, one can immediately compute the parameter $k_{react,on}$ required in simulations. In view of (10), the expected number of binding events per time and filament binding site is given by the on-rate $k_{react,on}$ times the number of linkers in the reaction volume of a certain binding site, which is $[L]V_{react}$. To get the total number of binding events per volume, one has to multiply this term with the concentration of filament binding sites per volume, i.e., with $[F]$, which leads to

$$k_{react,on}[L]V_{react}[F] = k_{on}[L][F] \tag{13}$$

and thus

$$k_{react,on} = k_{on}/V_{react}. \tag{14}$$

With

$$k_{react,off} = k_{off}, \tag{15}$$

simulation parameters can then directly be determined from the experimentally measured on- and off-rates of the bimolecular reaction (12). It is emphasized that in order to get a simulation parameter $k_{react,on}$ consistent to the experimentally measured k_{on}, not the real reaction volume is required in (14), but just the one used in the simulations, which is always known.

In case that experimental results are available only for either k_{on} or k_{off}, the respective other rate constant can be computed according to [26] by

$$\frac{k_{react,on}}{k_{react,off}} = \exp\left(-\frac{\Delta G_{L+F\rightarrow LF}}{k_B T}\right) \tag{16}$$

if at least the binding energy $\Delta G_{L+F\rightarrow LF}$ for linker binding is known. If no experimental data is available for a certain linker-filament combination, MD simulations are another data source for on- and off-rates or binding energies.

At the end of this section, it seems worth comparing the above model for chemical interactions between linkers and filaments with previously published ones and discussing possible extensions.

In [7,8] a similar model for chemical interactions between filaments and linkers is proposed. There, however, chemical bonds are assumed not to form with some probability p_{on}, but rather always if the linker is in the reaction volume of the filament and both have a proper relative orientation. The definition of the proper relative orientation for the reaction to happen requires some geometric parameters and tolerances. These are hard to determine in practice by experiments or MD simulations, which is a serious drawback of this approach. Furthermore, this model implicitly assumes that motion of filaments and linkers can be simulated by a micromechanical model sufficiently exactly down to the length and time scale relevant for chemical reactions. In reality, however, chemical reactions often happen on much a faster time scale and are furthermore affected by geometric or electrostatic properties on much a smaller length scale than considered in a micromechanical model on filament level. These potential problems of the approach pursued in [7,8] were the motivation for the development of a new numerical model for chemical interactions between linkers and filaments in this article whose parameters can be determined straight forward from experimental data and which does not require the precise resolution of any events on length and time scales relevant for the chemical reaction process itself.

Another important difference between the finite element method introduced in this article and previously published approaches for the simulation of biopolymer networks is that our approach enables capturing the chirality of filaments and linkers and therefore features such as a chiral arrangement of binding sites on the filaments as well as mechanical torsion or anisotropic bending stiffness. It is emphasized that already in [7,8] it was tried to capture these features by means of a Frenet-Serret frame, but that the formalism developed there is actually mathematically incorrect in case of general deformation, because of the singularity of the Frenet-Serret frame for straight filaments. In fact, classical bead-spring discretizations as used in [7,8] are in general not suitable to model these physical details, but only bead-spring discretizations enriched by material triads. These, however, result in inefficient algorithms, which partially even suffer from numerical instability in case of general deformation owing to singularities [11–13]. Thus the finite element method introduced in this article is anyway preferrable over bead-spring methods if one wants to model mechanical and chemical effects related to chirality.

In order to further extend and improve the model of chemical interactions in finite element simulations, future work may address an incorporation of Bell's formula [26] in the computation of the chemical off-rate, and a generalization of the position of the binding sites so that they do not have to coincide with the nodes of the finite element discretization any longer, but can be situated on arbitrary points on the filaments.

5.2. Mechanical contact

Mechanical contact interactions between filaments and linkers – which are in physics textbooks and articles usually referred to as 'excluded volume effects' – entail kinematic constraints to filament and linker motion which can be accounted for as usual in finite element simulations [44]. Whether this is necessary, depends on the physical quantities and properties of biopolymer networks one is interested in. For example, the equilibrium thermodynamics of networks consisting of (infinitesimally) thin filaments and linkers is independent of contact interactions. For in thermodynamic equilibrium, the probability of a certain network configuration depends only on its free energy, and for infinitesimally thin filaments the difference between the free energy of a system with and without excluded volume effects is almost surely equal to zero. Thus simulations lead to the same result with and without excluded volume effects, but faster in the latter case, because the rearrangement of the network into some specific equilibrium architecture happens faster without the kinematic constraints imposed by contact interactions. Therefore their neglection is advisable in studies of the equilibrium thermodynamics of networks such as presented in Section 7.3. Similarly, contact interactions can be neglected in studies of the viscoelasticity of homogeneous-isotropic networks in the small deformation regime if linker length and density are chosen high enough in order to make sure that filaments interact at entanglement points rather by linker molecules than mechanical contact. Such a case is considered, e.g., in the example in Section 7.2.

Whereas in certain special cases such as the above described ones contact interactions may be neglected, in general they play an important role in biopolymer networks. They can be incorporated in the finite element approach described in this paper by means of deterministic external forces in the equations of motion (3) and (7). As linkers are typically much smaller than filaments, the volume of free and singly bound linkers may either be neglected completely in contact computations or modeled as ball around the linker center or binding site to which the linker is attached. Doubly bound linkers are represented by beam elements and their volume can be accounted for in contact computations accordingly. If free and singly bound linkers are neglected, contact can be modeled exclusively as what is referred to in finite element textbooks and articles as beam contact. In principle, the methods described there can be directly applied to biopolymer networks. For this article, a common penalty and augmented Lagrange method for beam contact were implemented and tested in the example desscribed in Section 7.4. The tests confirmed the in principal suitability of these methods for simulations of biopolymer networks, but revealed at the same time some deficiencies of the standard algorithms typically employed in this field for example with respect to contact detection: because of the high slenderness ratio of biopolymers (e.g., around 10^3 for actin), the deformation a filament segment experiences within one time step may be significantly larger than its diameter. Standard contact algorithms may therefore sometimes not even detect any contact if two filaments simply completely pass through each other within one time step without overlapping in any iteration step in between. This naturally limits the time step size and thereby the efficiency of the simulations in general. The development of reliable and efficient remedies for such problems goes beyond the scope of this article, but is definitely a promising avenue of future research.

6. Multiscale simulations

The above introduced method for micromechanical simulations of biopolymer networks can be used alone or as part of a framework for multiscale simulations. There are various ways how to do so and in the following we will discuss in more detail only two simple ones, namely, a coupling to atomistic and MD simulations on the one hand, and a coupling to macroscopic continuum models on the other hand.

One can couple the above micromechanical model to atomistic and MD simulations in order to resolve processes even on an atomistic scale, but to keep the overall computational cost for the simulation of a large biopolymer network still moderate. To this end, atomistic and MD simulations are applied only at the few spots where a resolution below the micrometer scale significantly improves the accuracy. This is especially the case in the region where aggregation or disaggregation of chemical bonds happens. Both events are triggered by processes on a time and length scale way below the micrometer

and second scale usually considered in simulations of biopolymer networks. Resolving these processes in detail by means of MD simulations of the very neighbourhood of all spots where a linker and a filament binding site are close to each other may allow for much more realistic simulations than the coarse model of chemical reactions introduced in Section 5.1. Furthermore, MD simulations can be exploited in order to capture more details of polymer elasticity. In [28–30], beam models of polymers are considered only together with linear elastic constitutive laws. However, it is well-known that plasticity in form of folding and unfolding of certain protein domains play a major role for biopolymers in some cases. Again, these events are triggered by the structure of the polymers on a length scale way below the micrometer scale. Atomistic or MD simulations could be coupled to our micromechanical model wherever the critical tension for folding and unfolding is exceeded in the polymer. This way, one could drastically improve the accuracy of our simlutions without a major increase of the computational cost on the level of whole networks.

Macroscopic continuum simulations of biopolymer networks suffer from the severe problem that the macroscopic mechanical properties of biopolymer networks may change dramatically owing to micromechanical processes such as reorganization processes of the network architecture [45] which cannot be captured straightforward by any so far proposed constitutive law. This could be captured by coupling micromechanical simulations as shown in this article to macroscopic continuum models, e.g., at each Gauss point of the macroscopic models. We have recently proposed such an approach that works for three dimensional problems and is able to model complex processes on the macroscale [46].

This way constitutive laws for the macroscopic model could be determined bottom-up and the effects of processes on filament scale could be naturally incorporated into the macroscopic models. In Sections 7.2 and 7.3 it will be shown how both the network architecture and the macroscopic viscoelastic moduli can be determined by micromechanical simulations of biopolymer networks. This can be exploited, e.g., for the simulation of processes in tissue engineering and in the long run perhaps also cancer therapy. To this end, one can model cells on cellular scale scale as continua whose mechanical properties at different points in space can be resolved in detail by additional micromechanical simulations of the cytoskeleton in the cells with the method introduced in this article.

7. Examples

7.1. General

In the following section, a series of examples will be presented for validation and verification of the above introduced approach for the simulation of biopolymer networks. In this section, all numerical values are given in terms of the basis units micrometer, second, miligram and Kelvin if no other units are indicated explicitly. By default, temperature is set in the following examples to $T = 296.15$, thermal energy to $k_BT \approx 4.0889\text{e}{-3}$, which is equivalent to room temperature, fluid viscosity to $\eta = 1\text{e}{-3}$, which is equivalent to the one of water at room temperature, the fluid velocity fields to $\boldsymbol{v} = \boldsymbol{0}$ and $\boldsymbol{\omega} = \boldsymbol{0}$. For the filaments we chose as default values: cross section $A = 1.9\text{e}{-7}$, Young's modulus $E = 1.3\text{e}9$, Poisson ratio $v = 0.3$, moment of inertia of area perpendicular to the polymer axis $I = 2.8\text{e} - 11$, polar moment of inertia of area $J = 5.7\text{e} - 11$, translational friction coefficient per unit length parallel to the polymer axis $\gamma_{t\parallel} = 6.3\text{e}{-3}$, translational friction coefficient per unit length perpendicular to the polymer axis $\gamma_{t\perp} = 1.3\text{e} - 2$, rotational friction coefficient per unit length about the polymer axis $\gamma_{r\parallel} = 4.0\text{e} - 5$. For the linkers, we choose as default values: cross section $A_{cl} = 2.4\text{e} - 5$, Young's modulus $E_{cl} = 2.6\text{e}6$, Poisson ratio $v_{cl} = 0.3$, moment of inertia of area perpendicular to the polymer axis $I_{cl} = 4.5\text{e} - 11$, polar moment of inertia of area $J_{cl} = 9.0\text{e} - 11$, linker length $R_{cl} = 0.1$, linker length tolerance $\Delta R_{cl} = 0.02$, translational friction coefficient per unit length parallel to the polymer axis $\gamma_{t\parallel,cl} = 6.3\text{e} - 3$, translational friction coefficient per unit length perpendicular to the polymer axis $\gamma_{t\perp,cl} = 1.3\text{e} - 2$, rotational friction coefficient per unit length about the polymer axis $\gamma_{r\parallel,cl} = 4.0\text{e} - 5$. The above parameters were determined as follows: filament parameters were in general adopted from the case 'actin alone' in Tables C.1 and C.2 of [47]. In [8] it was found that axial stiffness of actin filaments plays only a minor role for networks without prestretch and that in this case therefore an artificially slightly decreased extensional stiffness parameter is a good choice for numerical simulations, because it does not alter the mechanical behavior perceptibly and yet renders at the same time the problem numerically more convenient. Following the argumentation in [8], also we used in the present article as default value a slightly reduced filament cross section as compared to Tables C.1 and C.2 of [47]. For similar reasons we furthermore employed a slightly increased rotational friction coefficient $\gamma_{r\parallel}$ after having confirmed the small influence of this parameter to this physics studied in the examples below. Owing to a lack of data from experiments or MD simulations, the linker cross section could be chosen only heuristically in such a way that linkers were almost inextensible in axial direction, but quite soft towards torsion and bending, which is in good accordance with what is generally assumed by experimentalists for long linkers such as filamin whose length from Table 1 is used as linker length. Linker friction coefficients were computed according to the equations given in [30] from their length and the viscosity of the surrounding fluid.

The equation system in the implicit Euler scheme is solved with the PTC method introduced in [30] with the parameters $c_{PTC,trans,1} = 0$, $c_{PTC,rot,1} = 0.145$, and $\alpha_{PTC} = 6.0$. In general, simulations start with straight filaments. Theories in polymer physics, however, often assume an equilibrated configuration as starting point, which is a configuration where filaments have already undergone a stochastic bending deformation characteristic for the respective temperature. Therefore in Section 7.2 and 7.3 simulation data is analyzed only after an initial equilibration time $\tau_{bend} \approx (\gamma_{t\perp}/EI)(L/\pi)^4$, which is the characteristic time constant of the slowest bending eigenmode of a filament with length L [26], and therefore the span on time filaments

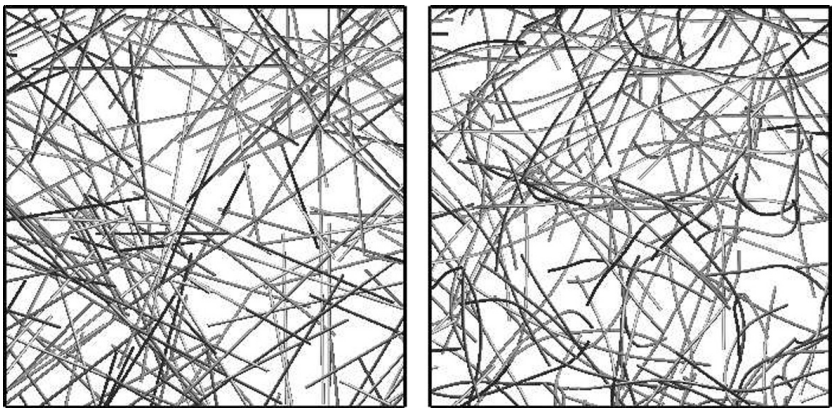

Fig. 3. Initial configuration at point in time $t = 0$ (left) and configuration at $t = \tau_{bend}$: at $t = \tau_{bend}$ filaments are not only randomly distributed, but also stochastically ondulated thereby representing a typical thermal equilibrium configuration.

need to reach a configuration characteristic for thermal equilibrium (cf. Fig. 3). For all examples, simple periodic boundary conditions are used except for the one in Section 7.2. Here, simple periodic boundary conditions are only used in x_1- and x_2-direction. At the x_3-boundaries of the simulation volume, periodic boundary conditions are combined with a sinosoidal Dirichlet condition imposed on the filaments causing a shear deformation of the network.

7.2. Viscoelasticity of permanently cross-linked actin networks

The cytoskeleton in biological cells is a biopolymer network mainly consisting of actin filaments, intermediate filaments and microtubules. In order to explore the physical foundations of the cytoskeleton, often pure actin networks are studied as model systems with different kinds of linkers. The viscoelastic properties of such networks have attracted significant attention in the last years (cf. [49] for recent references). Clearly, the computational analysis of the viscoelasticity of actin networks is an important application for the model developed in this article. A comprehensive and general numerical study of the viscoelasticity of actin networks goes by far beyond the scope of this paper. However, in this section at least the general capability of the simulation model introduced above to capture this viscoelasticity on a micromechanical scale will be demonstrated. To this end, the storage modulus G^* and loss modulus G^{**} of an actin-rigor-HMM network with glutaraldehyde measured experimentally [48] are compared to the ones observed in computer simulations based on our novel computational approach. Glutaraldehyde serves here in order to prevent the chemical bonds between actin and rigor-HMM from breaking up so that once established cross-links between actin filaments become permanent. As compared to the default values given in Section 7.1, friction coefficients were chosen by a factor 18 smaller, in order to account for the decreased drag forces and moments due to hydrodynamic interactions. As no accurate theories for hydrodynamic interactions in networks are available so far, this factor has been determined just by fitting experimental data. It is underlined that the applied default value for R_{cl} is 2.5 times larger than indicated for HMM in Table 1 in order to compensate for the fact that the distance between the filament binding sites in the simulation is $h = 0.125$ and therefore also much larger than in reality. Chemical interactions between filaments and linkers are governed by the parameters $\phi = \pi/4$, $\Delta\phi = \pi/4$, $k_{react,on} = 1e13$, and $k_{react,off} = 2$. The latter on- and off-rates are used only in the beginning of the simulations until the altogether $n_{cl} = 1400$ linkers in the simulation volume have formed a great number of crosslinks between the filaments. Subsequently, both are set to zero so that no further chemical bonds are formed or destroyed. This way, the effect of glutaraldehyde is mimicked which prevents chemical bonds between actin and rigor-HMM from breaking up so that in the beginning, rapidly a great number of chemical bonds is formed which than remains stable. The overly high on-rate in the beginning is used in order to accelerate the formation of chemical bonds so that the network reaches an equilibrium configuration in a shorter span on time.

The computer simulation is performed with time step sizes within the interval $\Delta t \in [4e-5; 1e-3]$ – small time steps for high load frequencies and large time steps for low load frequencies – in the cubic simulation volume $[0;4] \times [0;4] \times [0;4]$. In x_1- and x_2-direction, periodic boundary conditions are applied. In x_3-direction, a sinosoidal shear deformation $\boldsymbol{u}$ is imposed to the network by a Dirichlet condition with $u_2 = u_3 = 0$ and

$$u_1(\boldsymbol{x}, t) = \begin{cases} 0.08 \sin 2\pi f t & \text{if } x_3 = 4 \\ 0 & \text{if } x_3 = 0, \end{cases} \tag{17}$$

where f is the oscillation frequency of the shear deformation. This shear deformation entails in the background fluid the velocity fields

$$\boldsymbol{v} = \frac{\dot{u}_1}{5} \begin{pmatrix} 0 & 0 & 1 \\ 0 & 0 & 0 \\ 0 & 0 & 0 \end{pmatrix} \boldsymbol{x}. \quad \boldsymbol{\omega} = \boldsymbol{0}. \tag{18}$$

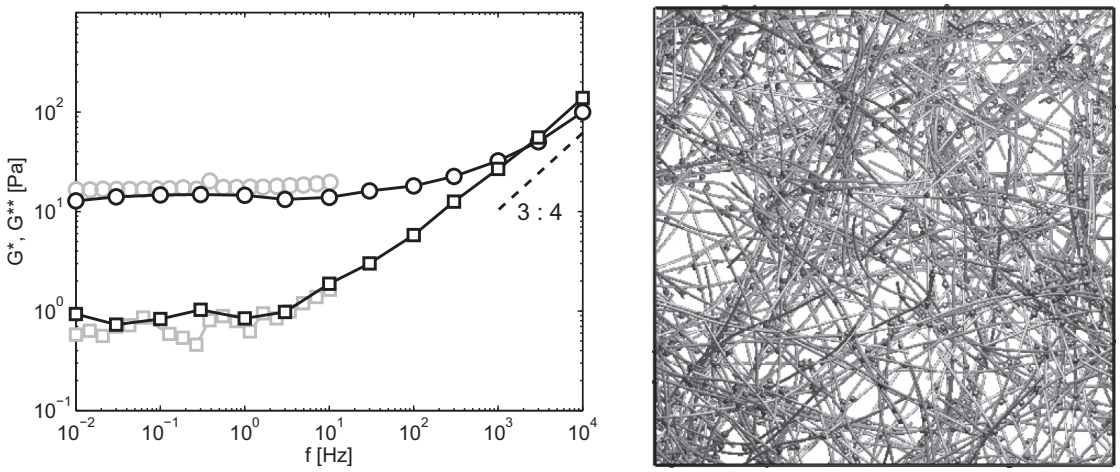

Fig. 4. Comparison (left) between storage (circles) and loss (squares) moduli observed in simulations (black) and experiments (grey, [48]) and theoretically predicted 3/4-slope for high frequencies (dashed line); simulated actin-rigor-HMM network with glutaraldehyde (right).

Fig. 4 shows good agreement between experiments and computer simulations up to 10 Hz. For frequencies higher than 10 Hz, no experimental data is available. However, in the limit of very high frequencies theorists [50] predicted a 3/4-slope for G^{**} and G^{*}. This slope is obviously reproduced correctly by the simulations for G^{**} beyond 10^3 Hz, and also G^{*} seems to approach it more and more in the limit of very high frequencies. Fig. 4 clearly demonstrates the capacity of the micromechanical model developed in this article to capture macroscopic material properties of biopolymer networks such as their viscoelastic moduli. It is underlined that previously published models are not suitable for the low frequency regime examined in this example owing to their tremendous computational cost. For example, the bead-spring model used in [8] enabled simulations only down to a load frequency of $f = 1Hz$ and even this only at an excessive computational cost (cf. Section 7.4). In contrast, with the simulation model developed in this paper, computational studies also in the low frequency regime far below $1Hz$ are possible. This is especially important, because many biologically relevant processes in biopolymer networks happen on the length scale 1–10 μm and time scale $10–10^3$ s. To the authors' knowledge the proposed numerical method is the first one suitable for these scales.

7.3. Structural polymorphism

Structural polymorphism is well-known to largely determine the viscoelasticity of living cells [45]: in a variety of experiments (see [49] for recent references) different super-structures have been observed in biopolymer networks which may arise instead of a simple homogeneous, isotropic network architecture. Namely, bundles [51], clusters [45] and layers [52] have been observed, whereas in theoretical studies [53] bundles and cubatic structures were predicted. A strong dependency of different network structures on certain crosslinker properties has been hypothesized. Yet, the difficulties in manipulating single properties of crosslinkers molecules and setting them to taylor-made values have rendered it so far impossible to verify these hypotheses by experiments. In this section we briefly demonstrate the possibilities the computational framework introduced in this article offers in this field: we simulated in a cubic volume of edge length $H = 5$ a network of actin biopolymers with a filament concentration $c_a = 4$ μM at room temperature. All filaments were supposed to have the length $L = 4$, and linker cross section was chosen as $A_{cl} = 4.8e-6$. All other filament and linker parameters were chosen identical to the default parameters in Section 7.1. Simulation time step size and spatial discretization length were set to $\Delta t = 0.01$ and $h = 0.125$. Depending on the concentrations and different physical properties of filaments and linkers, e.g., the orientation constraints for cross-linking defined by ϕ and $\Delta\phi$, homogeneous-isotropic networks, bundles, clusters and layers were observed in the computer simulations, i.e., exactly the network architectures observed also in experiments. These simulation results are illustrated in Fig. 5 and demonstrate that the computational method introduced in this article is suitable for numerical studies of the structural polymorphism of biopolymer networks. A comprehensive such study clarifying exactly the effect of the different physical properties of linkers and filaments to the structural polymorphism will be presented in future work.

7.4. Computational performance

Since the 1960s so-called bead-spring models have been applied in computational polymer physics for BD simulations, usually together with an explicit Euler time integration scheme. In [7,8], this approach is employed for micromechanical computer simulations of actin networks. In this section, the efficiency of this approach and the finite element approach developed in this article are compared. The simulation of a 12 μM actin network in a cube with edge length 2.8 over the span on time $t_{max} = 1$ is reported in [8] to take approximately 16 days on a single core of an Intel Xeon 2.66 GHz CPU with a

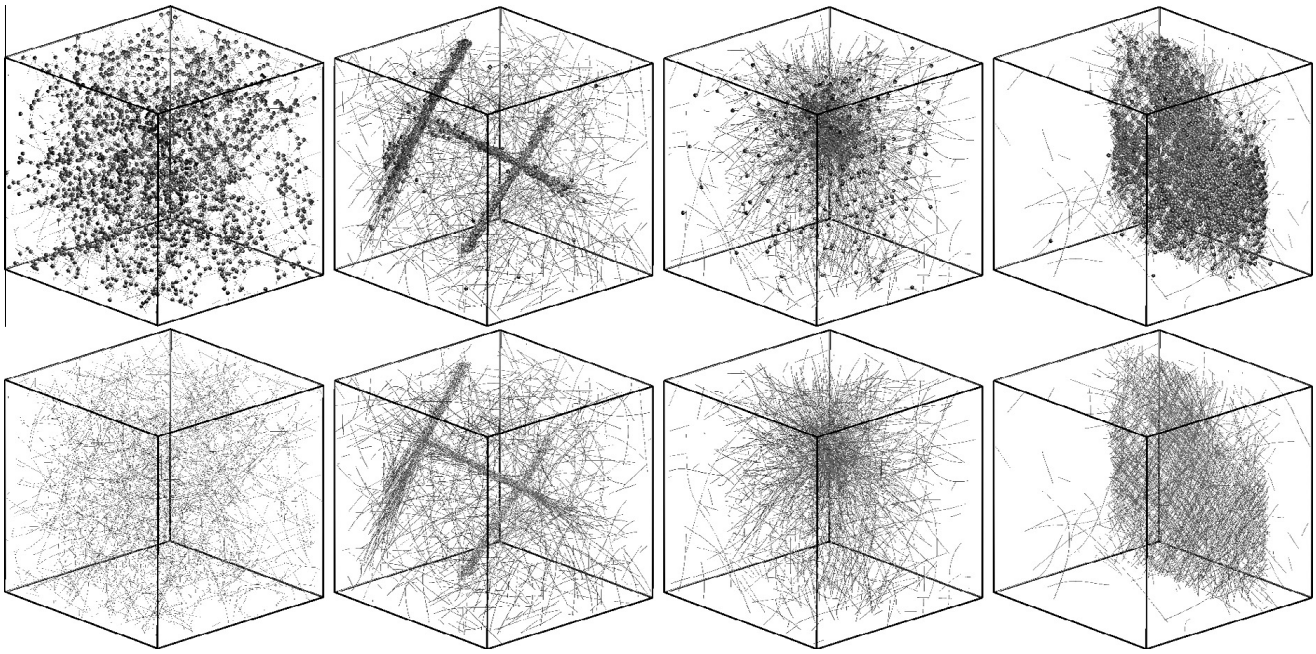

Fig. 5. Isotropic, bundle, cluster and layer (from left to right) network phase reproduced in a finite element simulation of a 4 μM actin network, illustrated with (top) and without (bottom) crosslinker molecules.

classical bead-spring model. A system with identical physical parameters was simulated with the finite element method developed in this article. There, the discretization length h was chosen equal to the one of the bead-spring discretization employed in [8]. The parallel rotational friction coefficients and the Poisson ratios, which do not exist in bead-spring discretizations, were set to $\gamma_{r\|} = \gamma_{r\|,cl} = 7.3e-4$ and $\nu = \nu_{cl} = 0.3$, and excluded volume effects were accounted for by means of an augmented Lagrange method with overlap tolerance 5e−4. On a single core of an Intel Core2 Quad Q6600 2.40 GHz CPU, which exhibits approximately the same performance as the hardware employed in [8], the finite element simulation took only 325 min and was therefore 71 times – i.e., roughly two orders of magnitude – faster than the bead-spring simulation shown in [8]. The superior performance of the finite element method is even underlined by the fact that in [8] a code tailor-made for bead-spring simulations of biopolymer networks was employed whereas the finite element simulation was conducted in the multipurpose in-house code BACI of the Institute for Computational Mechanics of the Technische Universität München. As a critical remark, it seems worth underlining that it is a deficiency of the above performance comparison that both simulation methods were not tested on one and the same hardware and operating system. The assumption that the computing power provided by the respective different environments in which the two methods were tested was comparable can be verified only roughly by public standard benchmarks such as Geekbench. However, in view of the overwhelming performance difference found, it seems acceptable neglecting the minor inaccuracies introduced thereby.

To a great extent, the low computational cost of the finite element simulation can definitely be explained by the fact that the implicit Euler scheme allows for a time step size 4.86e5 times larger than the explicit scheme used in [8]. Therefore an important question is whether a bead-spring model with the same implicit Euler scheme might not be even more efficient

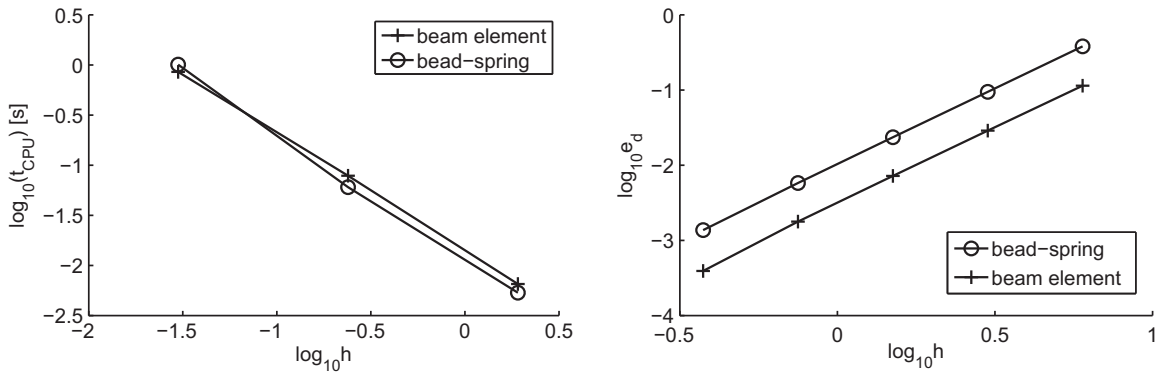

Fig. 6. Comparison between finite beam elements according to Section 17.2 from [54] and bead-spring model: CPU time t_{CPU} for simulation of single, free actin filament with time step size $\Delta t = 1e-5$ and spatial discretization length h over total time $t_{max} = 10$ (left); convergence of the displacement error e_d at the center of a simply supported beam under central point force (right).

due to the simplicity of bead-spring models as compared to finite element models. Fig. 6 demonstrates, however, that the computational cost of a discretization with finite beam elements is comparable to the one of a bead-spring discretization for an implicit Euler scheme, and that it achieves at the same time an accuracy by a factor of 4 higher. At the same time, finite elements offer a variety of additional benefits such as material triads allowing for a consistent torsion model and a detailed model of the geometry of chemical binding sites. In addition to that, it is underlined that here only finite elements based on Reissner's beam theory are discussed. However, owing to the high slenderness ratios of many biopolymers, nonlinear Euler–Bernoulli beam elements are actually expected to be even more accurate and efficient – the only reason why such elements are not considered in this paper is that to the author's knowledge no fully nonlinear geometrically exact Euler–Bernoulli beam element has been developed and published so far. Altogether, these arguments clearly reveal that finite elements are more suitable for the spatial discretization of filaments in biopolymer networks and have much a greater potential in the future than bead-spring models.

8. Conclusions

In this article we introduced a framework for micromechanical simulations of biopolymer networks with finite beam elements. To this end the filaments, linkers and fluid in the network are modeled as continua, respectively. This micromechanical point of view allows for a resolution of processes down to the micrometer length scale, which is generally assumed to be the most relevant one for the mechanics of such networks. This way it enables much more detailed analyses of biopolymer networks than macroscopic continuum models do, where the whole network is just considered as a bulk with a suitable material law. On the other hand and in opposition to Molecular Dynamics simulations, the computational cost of our approach still allows for the simulation of systems on the biologically most relevant length scale 1–10 μm and time scale $10–10^3$ s. In opposition to various previous micromechanical models of biopolymer networks based on finite elements [5,2–4], our approach captures also effects of non-equilibrium statistical mechanics. This has been possible so far only by means of heuristic filament discretizations such as bead-spring models and at a tremendous computational cost [7,8]. In contrast to that, the finite element discretization of the filaments we use can be derived from first principles of Newtonian and statistical mechanics in a stringent mathematical way and results together with a backward Euler time integration scheme in algorithms which are approximately two orders of magnitude faster than state-of-the-art methods such as bead-spring models. This way, the approach we described above allows for addressing problems no other numerical method could deal with so far, especially the analysis of the viscoelastic low frequency regime of biopolymer networks or of their structural polymorhpism.

The framework we introduced in this article is essentially based on the discretization of biopolymers with finite beam elements and a backward Euler time integration scheme. Therefore it can be implemented quickly in already existing finite element codes. All these advantages give reason to the hope that the finite element approach introduced in this article has the potential to completely substitute traditional approaches such as bead-spring models in the simulation of biopolymer networks in the medium term.

As pointed out in Section 6, the simulation approach discussed in this article can not only be used alone, but also in various ways for multiscale simulations: on the one hand, it can be enriched by information gained from additional atomistic or MD simulations about processes on smaller length and time scales. On the other hand, simulations on filament level as discussed in this article can be used as information source for coarser continuum models allowing for simulations of very large systems. For example, on cellular scale, processes in tissue engineering or in the long run perhaps also cancer therapy could be simulated modeling each cell as a mechanical continuum, and information about the mechanical properties of these continua at different points in space could be determined by additional micromechanical simulations of the cytoskeleton with the framework introduced in this article. This way, coupled simulations on cellular and subcellular scale could enable detailed and realistic computer models of multi-cell systems.

Acknowledgements

The support of the first (C.J.C.) and second (K.W.M.) author by the International Graduate School of Science and Engineering (IGSSE) of the Technische Universität München ist gratefully acknowledged. Furthermore we thank Professor Robijn Bruinsma from the University of California Los Angeles for fruitful discussions.

References

[1] J.S. Palmer, M.C. Boyce, Constitutive modeling of the stress-strain behavior of f-actin filament networks, Acta Biomater. 4 (2008) 597–612.
[2] C. Heussinger, E. Frey, Eur. Phys. J. E: Soft Matter 24 (2007) 47–53.
[3] E.M. Huisman, T. van Dillen, P.R. Onck, E. Van der Giessen, Three-dimensional cross-linked f-actin networks: Relation between network architecture and mechanical behavior, Phys. Rev. Lett. 99 (2007) 208103–208104.
[4] P.R. Onck, T. Koeman, T. van Dillen, E. van der Giessen, Alternative explanation of stiffening in cross-linked semiflexible networks, Phys. Rev. Lett. 95 (2005) 178102.
[5] J.A. Åström, P.B.S. Kumar, Strain hardening, avalanches, and strain softening in dense cross-linked actin networks, Phys. Rev. E 77 (2008) 051913.
[6] J.R. Blundell, E.M. Terentjev, The influence of disorder on deformations in semiflexible networks, Proc. R. Soc. A (2011) rspa.2010.0600v1–rspa20100600.
[7] T. Kim, W. Hwang, R. Kamm, Computational analysis of a cross-linked actin-like network, Exp. Mech. 49 (2009) 91–104.

[8] T. Kim, W. Hwang, H. Lee, R.D. Kamm, Computational analysis of viscoelastic properties of crosslinked actin networks, PLoS Comput. Biol. 5 (2009) e1000439.
[9] P.L. Chandran, M.R.K. Mofrad, Rods-on-string idealization captures semiflexible filament dynamics, Phys. Rev. E 79 (2009) 011906.
[10] E.M. Huisman, C. Storm, G.T. Barkema, Frequency-dependent stiffening of semiflexible networks: A dynamical nonaffine to affine transition, Phys. Rev. E 82 (2010) 061902.
[11] G. Chirico, Torsional-bending infinitesimal dynamics of a dna chain, Biopolymers 38 (1996) 801–811.
[12] G. Chirico, J. Langowski, Kinetics of dna supercoiling studied by brownian dynamics simulation, Biopolymers 34 (1994) 415–433.
[13] H. Wada, R.R. Netz, Hydrodynamics of helical-shaped bacterial motility, Phys. Rev. E 80 (2009) 021921.
[14] A. Montesi, D.C. Morse, M. Pasquali, Brownian dynamics algorithm for bead-rod semiflexible chain with anisotropic friction, J. Chem. Phys. 122 (2005) 084903–084908.
[15] Reproduced with permission from International Journal for Numerical Methods in Engineering (2011), Copyright 2011 John Wiley & Sons, Ltd.
[16] M. Doi, S.F. Edwards, The theory of polymer dynamics, Clarendon Press, Oxford, 1994.
[17] E.H. Hauge, A. Martin-Löf, Fluctuating hydrodynamics and brownian motion, J. Stat. Phys. 7 (1973) 259–281.
[18] D.L. Ermak, J.A. McCammon, Brownian dynamics with hydrodynamic interactions, J. Chem. Phys. 69 (1978) 1352–1360.
[19] J. Rotne, S. Prager, Variational treatment of hydrodynamic interaction in polymers, J. Chem. Phys. 50 (1969) 4831–4837.
[20] P.L. Chandran, M.R.K. Mofrad, Averaged implicit hydrodynamic model of semiflexible filaments, Phys. Rev. E 81 (2010) 031920.
[21] M.W. Gee, U. Küttler, W.A. Wall, Truly monolithic algebraic multigrid for fluid-structure interaction, Int. J. Numer. Methods Eng. 85 (2010) 987–1016.
[22] L.L. Goff, O. Hallatschek, E. Frey, F. Amblard, Tracer studies on f-actin fluctuations, Phys. Rev. Lett. 89 (2002) 258101.
[23] X. Liu, G.H. Pollack, Mechanics of f-actin characterized with microfabricated cantilevers, Biophys J. 83 (2002) 2705–2715.
[24] Y. Tsuda, H. Yasutake, A. Ishijima, T. Yanagida, Torsional rigidity of single actin filaments and actin–actin bond breaking force under torsion measured directly by in vitromicromanipulation, PNAS 93 (1996) 12937–12942.
[25] M. Wang, H. Yin, R. Landick, J. Gelles, S. Block, Stretching dna with optical tweezers, Biophys. J. 72 (1997) 1335–1346.
[26] J. Howard, Mechanics of Motor Proteins and the Cytoskeleton, Sinauer Associates, Sunderland, 2001.
[27] J.M. Deutsch, Internal dissipation of a polymer, Phys. Rev. E 81 (2010) 061804.
[28] C.J. Cyron, W.A. Wall, Finite-element approach to brownian dynamics of polymers, Phys. Rev. E 80 (2009) 066704.
[29] C.J. Cyron, W.A. Wall, Consistent finite-element approach to brownian polymer dynamics with anisotropic friction, Phys. Rev. E 82 (2010) 066705.
[30] C.J. Cyron, W.A. Wall, Numerical method for the simulation of the brownian dysnamics of rod-like microstructures with three dimensional nonlinear beam elements, Int. J. Numer. Methods Eng. 90 (2012) 955–987.
[31] H. Shin, K.R.P. Drew, J.R. Bartles, G.C.L. Wong, G.M. Grason, Cooperativity and frustration in protein-mediated parallel actin bundles, Phys. Rev. Lett. 103 (2009) 238102.
[32] L. Castellani, G. Offer, A. Elliott, E.J. O'Brien, Structure of filamin and the f-actin-heavy merofilamin complex, J. Muscle Res. Cell Motility 2 (1981) 193–202.
[33] M. Hosek, J.X. Tang, Polymer-induced bundling of f actin and the depletion force, Phys. Rev. E 69 (2004) 051907.
[34] O. Lieleg, I. Vladescu, K. Ribbeck, Characterization of particle translocation through mucin hydrogels, Biophys. J. 98 (2010) 1782–1789.
[35] I. Borukhov, R. Bruinsma, Raft instability of biopolymer gels, Phys. Rev. Lett. 87 (2001) 158101.
[36] R. Tharmann, Mechanical Properties of Complex Cytoskeleton Networks, Ph.D. thesis, Technische Universität München, 2007.
[37] R. Meyer, U. Aebi, Bundling of actin filaments by alpha-actinin depends on its molecular length., J. Cell Biol. 110 (1990) 2013–2024.
[38] T. Nishizaka, R. Seo, H. Tadakuma, K. Kinosita, S. Ishiwata, Characterization of single actomyosin rigor bonds: Load dependence of lifetime and mechanical properties, Biophys. J. 79 (2000) 962–974.
[39] J. Golji, R. Collins, M.R.K. Mofrad, Molecular mechanics of the -actinin rod domain: Bending, torsional, and extensional behavior, PLoS Comput. Biol. 5 (2009) e1000389.
[40] K.S. Kolahi, M.R. Mofrad, Molecular mechanics of filamin's rod domain, Biophys. J. 94 (2008) 1075–1083.
[41] D.S. Courson, R.S. Rock, Actin crosslink assembly and disassembly mechanics for alpha-actinin and fascin, J. Biol. Chem. 285 (2010) 26350–26357.
[42] W. Goldmann, G. Isenberg, Analysis of filamin and [alpha]-actinin binding to actin by the stopped flow method, FEBS Lett. 336 (1993) 408–410.
[43] S.B. Marston, The rates of formation and dissociation of actin-myosin complexes. effects of solvent, temperature, nucleotide binding and head-head interactions., Biochem. J. 203 (1982) 453–460.
[44] P. Wriggers, Computational Contact Mechanics, Wiley, New York, 2002.
[45] O. Lieleg, K.M. Schmoller, C.J. Cyron, Y. Luan, W.A. Wall, A.R. Bausch, Structural polymorphism in heterogeneous cytoskeletal networks, Soft Matter 5 (2009) 1796–1803.
[46] L. Wiechert, W.A. Wall, A nested dynamic multi-scale approach for 3d problems accounting for micro-scale multi-physics, Comput. Methods Appl. Mech. Eng. 199 (2010) 1342–1351.
[47] C.J. Cyron, Micromechanical continuum approach for the analysis of biopolymer networks, Ph.D. thesis, Technische Universität München, 2011.
[48] O. Lieleg, M.M.A.E. Claessens, Y. Luan, A.R. Bausch, Transient binding and dissipation in cross-linked actin networks, Phys. Rev. Lett. 101 (2008) 108101.
[49] O. Lieleg, M.M.A.E. Claessens, A.R. Bausch, Structure and dynamics of cross-linked actin networks, Soft Matter 6 (2010) 218–225.
[50] F. Gittes, F.C. MacKintosh, Dynamic shear modulus of a semiflexible polymer network, Phys. Rev. E 58 (1998) R1241.
[51] O. Lieleg, M.M.A.E. Claessens, C. Heussinger, E. Frey, A.R. Bausch, Mechanics of bundled semiflexible polymer networks, Phys. Rev. Lett. 99 (2007) 088102.
[52] G.C.L. Wong, A. Lin, J.X. Tang, Y. Li, P.A. Janmey, C.R. Safinya, Lamellar phase of stacked two-dimensional rafts of actin filaments, Phys. Rev. Lett. 91 (2003) 018103.
[53] I. Borukhov, R.F. Bruinsma, W.M. Gelbart, A.J. Liu, Structural polymorphism of the cytoskeleton: A model of linker-assisted filament aggregation, Proc. Nat. Acad. Sci. USA 102 (2005) 3673–3678.
[54] M.A. Crisfield, Non-linear Finite Element Analysis of Solids and Structures, Volume 2: Advanced Topics, Wiley, Chichester, 2003.